Hindawi
International Journal of Rotating Machinery
Volume 2022, Article ID 1944753, 16 pages
https://doi.org/10.1155/2022/1944753

Research Article

A Comparative Study of Impeller Modification Techniques on the Performance of the Pump as a Turbine

Abdulbasit Nasir,[1] **Edessa Dribssa**,[2] **Misrak Girma**,[1,3] **and Tamerat Demeke**[2]

[1]*Department of Mechanical Engineering, Addis Ababa Science and Technology University, P.O. Box 16417, Addis Ababa, Ethiopia*
[2]*School of Mechanical and Industrial Engineering, Addis Ababa Institute of Technology, Addis Ababa University, P.O. Box 385, Addis Ababa, Ethiopia*
[3]*Renewable Energy Center of Excellence, Addis Ababa Science and Technology University, P.O. Box 16417, Addis Ababa, Ethiopia*

Correspondence should be addressed to Abdulbasit Nasir; abdulbasitn1@gmail.com

Received 5 September 2022; Accepted 26 October 2022; Published 14 November 2022

Academic Editor: Yutaka Ohta

Copyright © 2022 Abdulbasit Nasir et al. This is an open access article distributed under the Creative Commons Attribution License, which permits unrestricted use, distribution, and reproduction in any medium, provided the original work is properly cited.

The extensive use of the pump as a turbine (PAT) for micro-hydropower applications has a significant value from economic and technical viewpoints. However, the unavailability of the characteristics curve and relatively lower efficiency are the two basic limitations when considering pumps for power-generating applications. In this paper, the performance of the PAT is analyzed using the computational fluid dynamics (CFD) software called Ansys CFX in conjunction with standard k-ε. Then, experiments were done to verify the results of the simulation. Measurement inaccuracy effects are also taken into account. The initial performance of the PAT is refined by controlling basic design parameters (i.e., increasing the number of impeller blades, decreasing blade thickness, blade tip rounding, and adjusting blade inlet angle). Additionally, a new modification method known as blade grooving is also introduced in this research. Finally, all listed modification techniques are applied simultaneously to achieve maximum performance. The output of the study confirms that the adopted modification techniques have a positive effect on performance improvement. When the number of impellers is increased, the power output is enhanced by 5.72%, and blade grooving provides the most efficiency improvement, i.e., 7.00%. But decreasing blade thickness has no remarkable impact on the performance; the power output and efficiency are improved by 1.24% and 2.60%, respectively. The maximum performance improvement was achieved when the modification techniques are applied simultaneously with 10.56 and 10.20 percent of power and efficiency increments, respectively. From the entire study, it can be concluded that the chosen design parameters have an important effect on stabilizing the internal flow, decreasing the required head, decreasing the hydraulic loss in the impeller, and increasing the overall performance. The study also helps to figure out which modification technique is the most practical.

1. Introduction

Nowadays, the development of green energy-based technology for sustainable growth is attractive to the world. Among them, micro-hydropower (MHP) schemes are a more effective and practical alternative for rural electrification [1]. But, utilization of MHP using custom-made turbines is challenging due to its high price, especially in countries that have a lower gross domestic product (GDP) [2]. Therefore, introducing PAT in the place of an expensive power generation unit to operate in a reverse way is an economic option in MHP plants [3]. Furthermore, the use of a PAT has various advantages over custom-made turbines, such as availability in local markets, less initial cost [4], and availability for an extensive range of

Table 1: Design parameters of the pump in direct mode.

Parameters	Numerical value	Parameters	Numerical value
Volume flow rate	24.5 m^3/h	Specific speed	16
Pressure head	16.5 m	Blade tip diameter	0.16 m
Efficiency	72%	Number of blades	6
Rotating speed	2900 rpm	Suction head	0 m
Maximum power	3 hp	Working fluid density	1000 kg/m^3

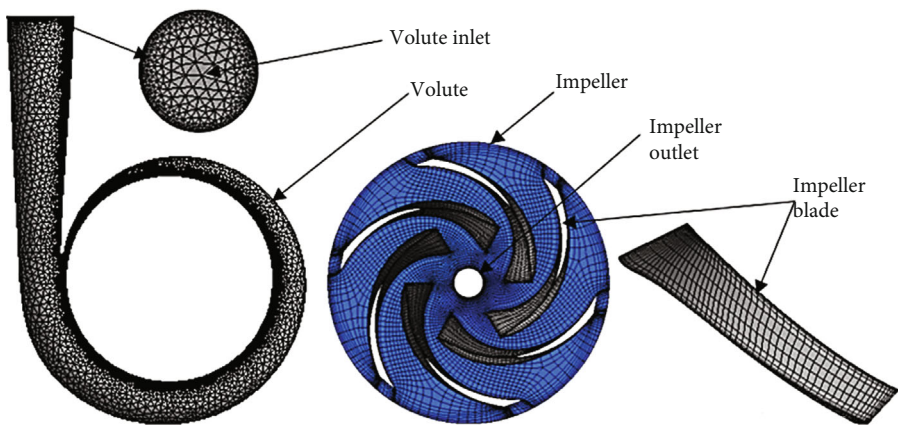

Figure 1: Mesh refinement in special areas.

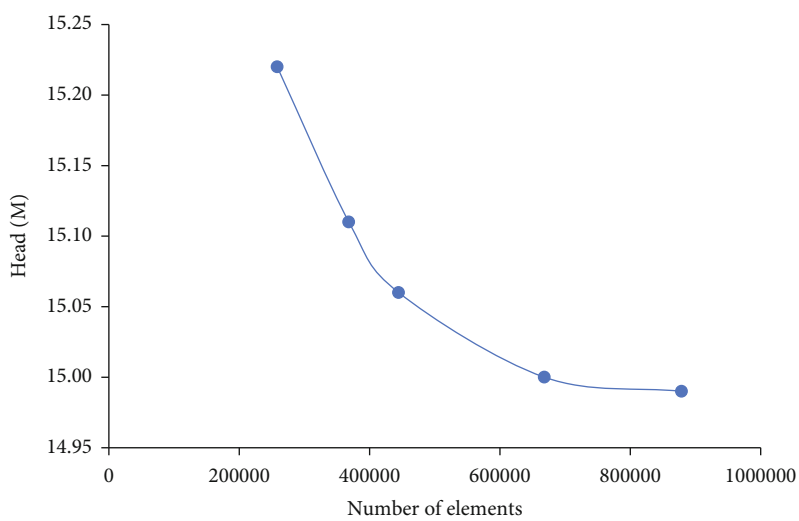

Figure 2: Effects of mesh number on the numerical result.

hydraulic data [5]. However, finding a characteristics curve for pump selection is not commonly available [6, 7]. Additionally, PATs have lower efficiency [8] when compared with Francis turbines [9] (frequently used for hydroelectric power generation) and cross-flow turbines [10] (mostly used in micro-hydropower systems in developing countries).

Previous studies have focused on PAT performance improvement by decreasing blade thickness, blade profile optimization, blade tip rounding, application of splitter blades, trimming impeller diameter, increasing the number of blades, and changing blade angles. Even though many scholars have worked on performance improvement, few research outputs are available on the multiple modification techniques. Singh and Nestmann [11] investigate the effects of impeller rounding on a combined radial and mixed flow pump as a turbine using experimental methods. In different

Table 2: Basic assumptions and settings used in the CFD analysis.

Steps	Parameters	Setting
Model	Solver	Pressure-based
	Space	Three-dimensional
	Time	Steady
	Turbulence model	Standard k-ε
Operating conditions	Operating pressure	101 kPa
	Gravitational acceleration	9.81 m/s^2 in Z-direction
	Density	997 kg/m^3
Material	Water	At standard working conditions
Boundary conditions	Inlet	Total pressure
	Outlet	Mass flow rate
	Interfaces	Specified between rotor and stator
	Impeller	Rotating wall
	Volute	Stationary wall

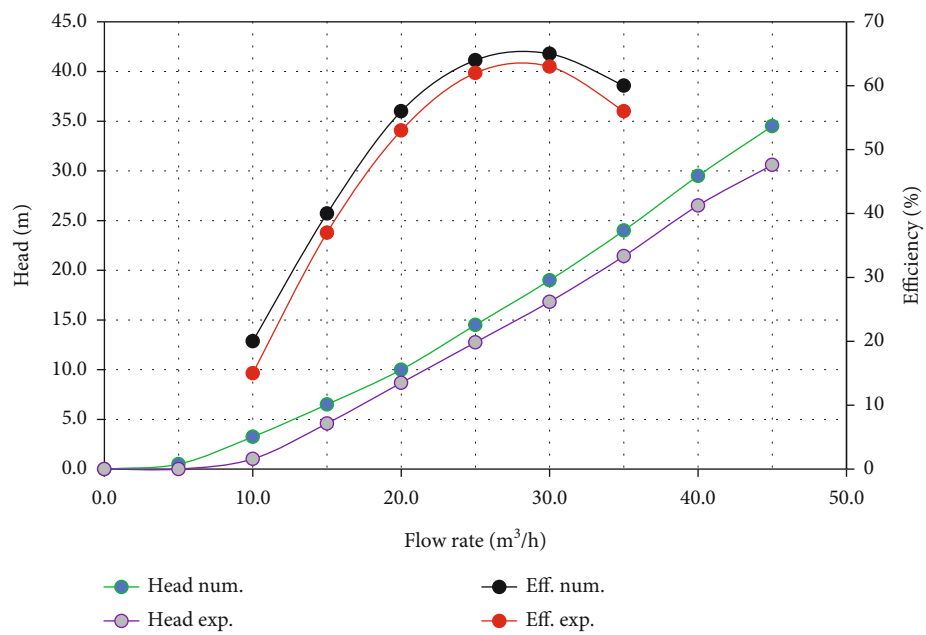

Figure 3: Comparison of numerical and experimental outputs.

operating regions, the result of the study showed a rise in efficiency by up to 3%. In the study of Han and Tan [12], the effect of rotating speed on energy performance, tip leakage flow, tip leakage vortex structure, and pressure fluctuation in a mixed flow pump is presented. The numerical and experimental result confirms that there is a direct proportion between the rotating speed and the performance of PAT. The study of Jianguo et al. [13] also confirms the efficiency of the pump as a turbine increases with increasing the rotational speed and the maximum output is achieved at 1500 rpm.

Yang et al. [14] carried out experimentation and numerical simulation on a single-stage centrifugal PAT, at impeller diameters of 255 mm, 235 mm, and 215 mm. The study revealed that flow rate and efficiency at the BEP decreased by 20 m^3/h and 2.17%, respectively, as the impeller diameter decreases from 255 mm to 215 mm. The output of the literature review, presented by Liu et al. [15], shows that impeller trimming has a negative impact on performance, but it is useful to adjust BEP. Ismail et al. [16] investigate the influence of the number of blades (5, 6, 7, and 8) on the performance of PAT. The simulation results showed that the highest efficiency was achieved at 7 blades with the efficiency taken at 76.24%. The effects of splitter blades were studied numerically by Sun-Sheng et al. [17]. After the application of splitter blades, the efficiency of PAT increased from

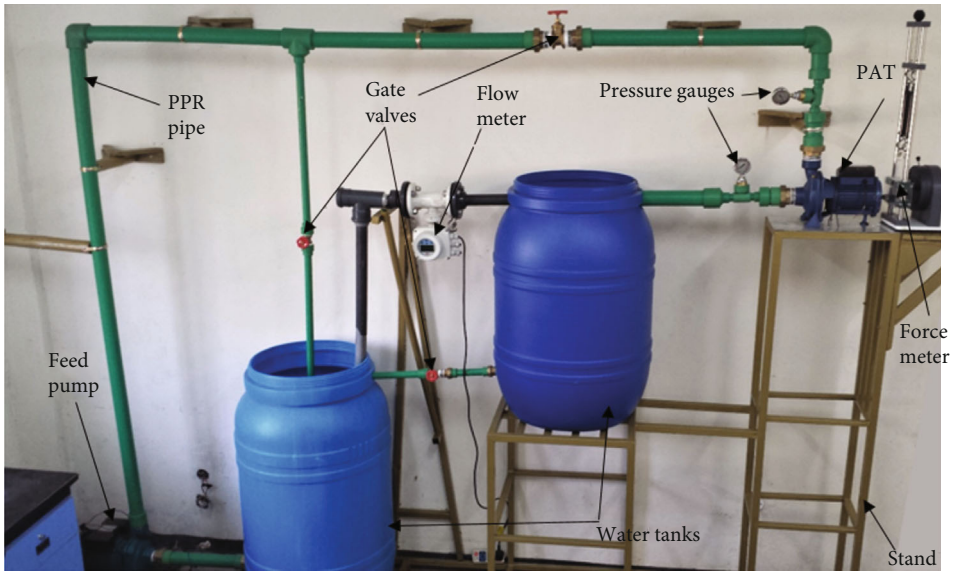

Figure 4: Experiment setup.

Table 3: Lists of measuring devices.

No.	Device	Dependent/independent parameter	Range	Error ± (%)
1	Electromagnetic flow meter	Flow rate (independent)	0-40 m^3/h	0.40
2	Pressure gauge	Pressure 1	0-16 bar	0.50
3	Pressure gauge	Pressure 2	0-16 bar	0.50
4	Digital contact tachometer	Rotational speed	0-4000 RPM	0.05
5	Force meter	Force	0-50 N	0.25
6	Total error equation (12)	—	—	0.85

Table 4: The deviation of CFD results at the BEP.

Measured parameter	Numerical result	Experimental result	Numerical error (%)
Head (m)	17.00	16.50	2.94
Flow rate (m^3/h)	27.50	28.00	-1.82
P_{out} (W)	850.33	825.85	2.88
Efficiency (%)	65.15	64.00	1.76

65.77% to 69.19%. Yang et al. [18] conducted a study on the influence of blade thickness on the performance of PAT. Numerical analysis was used, and the result indicates that the total hydraulic loss decreases and efficiency increases with decreasing blade thickness. This research also showed that blade angles and blade inlet width influence the performance of PAT.

Several serious research works were extensively conducted from a single modification technique. Unfortunately, the comparative study of different modifications was not widely addressed to find out the most effective one. Thus, this paper is aimed at introducing a novel modification technique called blade grooving and compared it with the recognized techniques such as increasing the number of blades, decreasing blade thickness, blade tip rounding, and changing the blade inlet angles. Then, those considered modification methods are applied simultaneously to achieve maximum performance. The external performance curve (flow capacity vs. pressure head, flow capacity vs. output power, and flow capacity vs. efficiency) and the inner flow fields are analyzed to evaluate the performance difference between initial and modified models.

2. Numerical Modelling

In the present study, a single-stage single-section commercially available centrifugal pump is considered, and Table 1 lists the pump parameters in detail. The performance

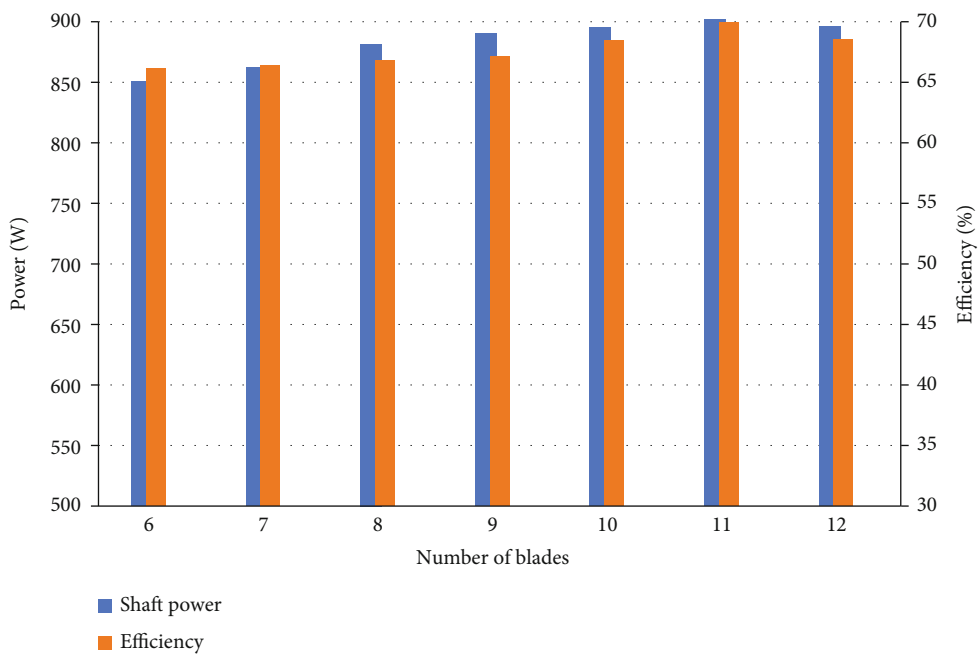

Figure 5: The effect of the number of impeller blades on the PAT performance.

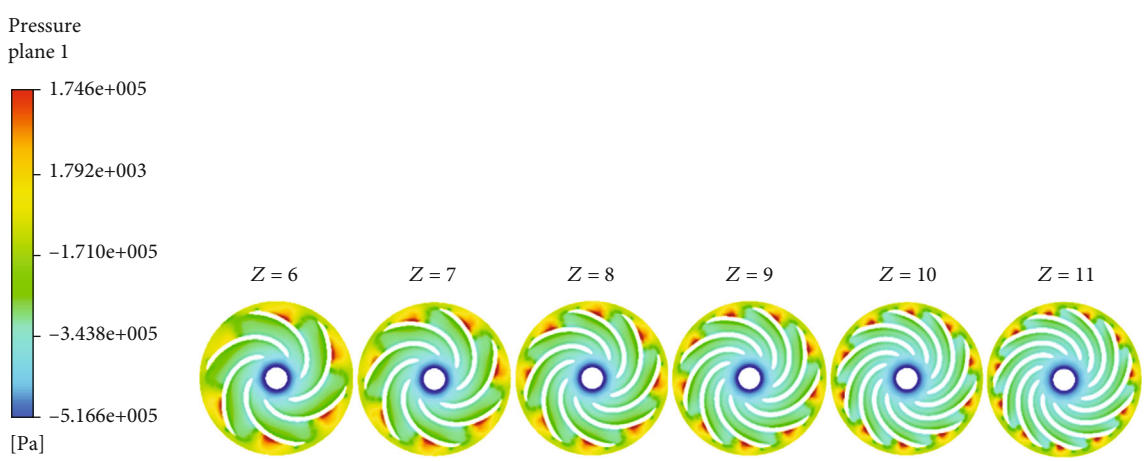

Figure 6: Pressure counters of the impeller in the middle section.

analysis and performance enhancement approaches for the model are discussed in the next section.

2.1. Geometry and Mesh Generation. A module called centrifugal pump design (Vista CPD) available in Ansys software is used to create a three-dimensional model of the PAT. Then, the blade of the pump was further modified by using BladeGen. Regular mesh with appropriate size was made by using the Ansys mesh tool for volute and turbomesh for the impeller (Figure 1). Mesh definition is essential to find stability among excessive grid sizes for acceptable correctness and a coarse mesh to decrease the computational time [19].

A grid dependency analysis was carried out to check whether the result depends on the grid size or not. The fifth grid size is increased by 31.5% concerning the fourth one, while the simulation result showed less than 0.05% (Figure 2). Therefore, the grid number of 7×10^5 cells was chosen to perform the numerical simulation.

2.2. Physics Setup. The physical model utilized in the solver was developed using the finite volume method (FVM) and a second-order spatial discretization scheme for the convection terms in the governing equations. The current model is governed by continuity and momentum equations. For the convergence condition, a relative error of less than 0.00001 is considered. The entire PAT is characterized using the standard k-ε turbulence model due to its robustness, quick convergence, and acceptable accuracy [20]. The conservation laws for mass and momentum in the Cartesian

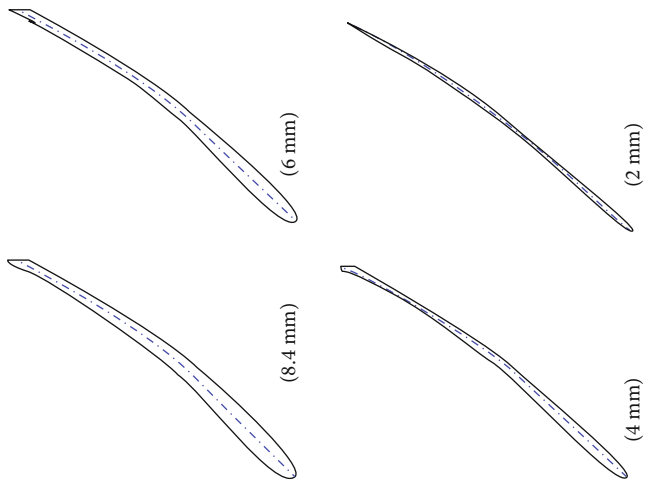

Figure 7: The disparities in blade thickness.

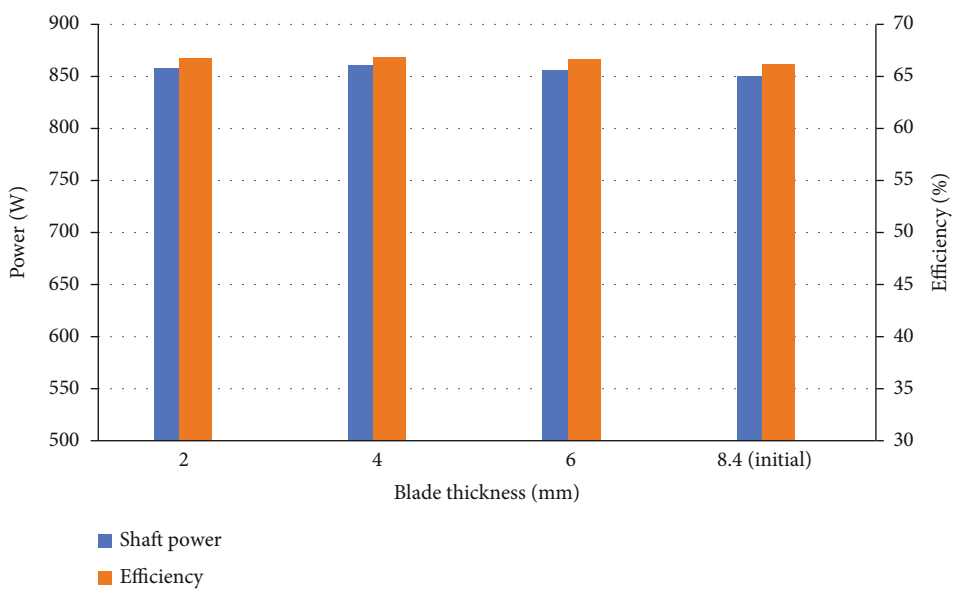

Figure 8: The effect of decreasing blade thickness on the power output and efficiency.

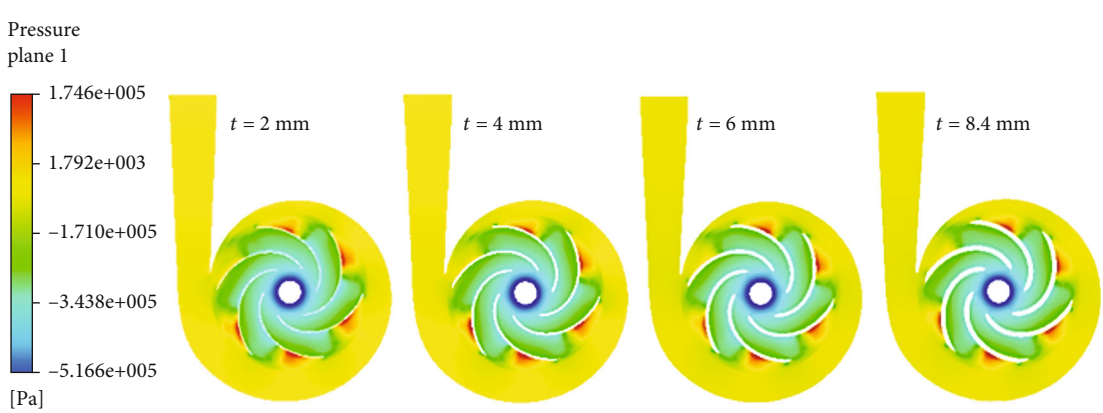

Figure 9: Pressure counters in the PAT impeller's center portion.

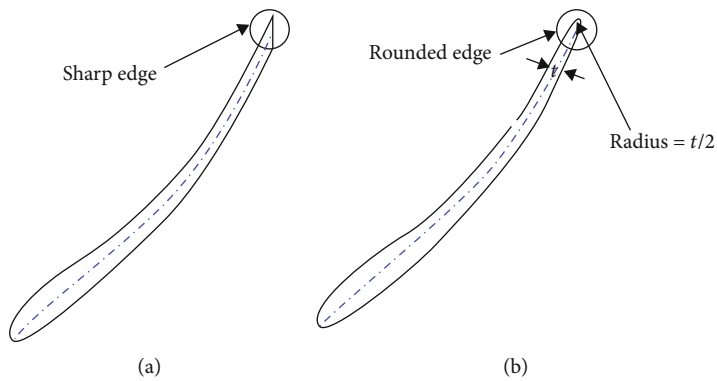

Figure 10: Blade tip rounding.

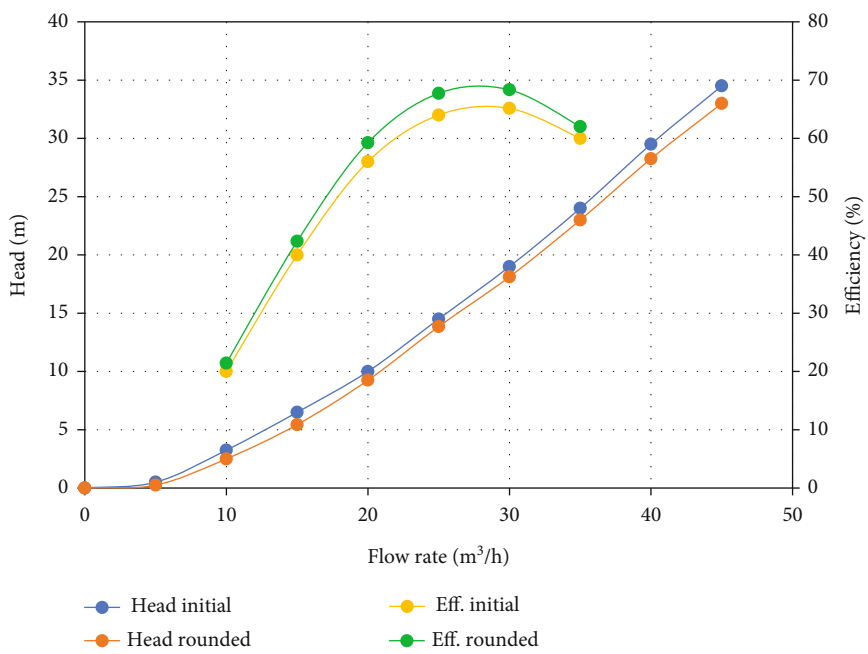

Figure 11: PAT performance and the influence of blade rounding.

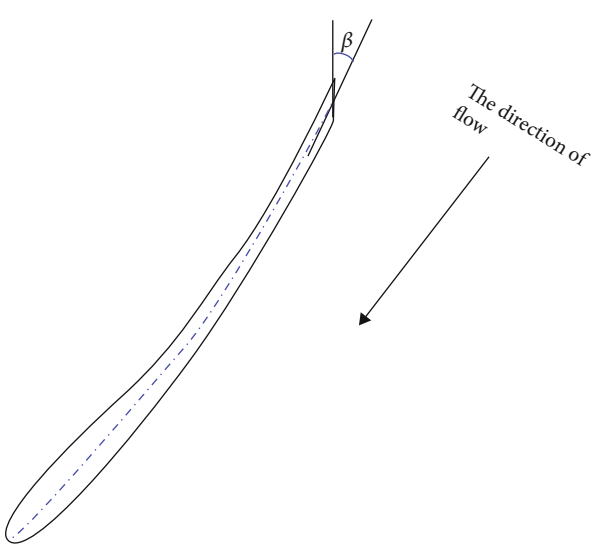

Figure 12: PAT blade inlet angle.

coordinate system rotating with angular velocity can be written in the conservation form as follows [21, 22]:

$$\frac{\partial \rho}{\partial t} + \frac{\partial}{\partial x_i}(\rho u_i) = 0, \tag{1}$$

$$\frac{\partial \rho u_i}{\partial t} + \frac{\partial}{\partial x_j}(\rho u_i u_j) + \frac{\partial p}{\partial x_i} = \frac{\partial}{\partial x_j}\left(\tau_{ij}\tau_{ij}^{R}\right), \tag{2}$$

where u is the fluid velocity, ρ is the fluid density, and τij is the viscous shear stress tensor; for Newtonian fluids, it is related to the strain rate by

$$\tau_{ij} = \mu\left(\frac{\partial u_i}{\partial x_j} + \frac{\partial u_j}{\partial x_i} - \frac{2}{3}\delta_{ij}\frac{\partial u_k}{\partial x_k}\right). \tag{3}$$

Following the Boussinesq assumption, the Reynolds

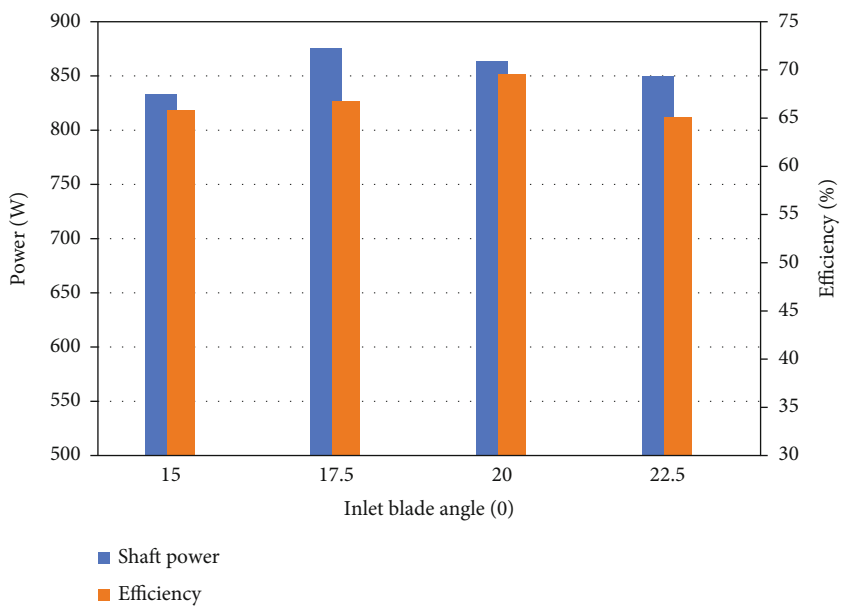

Figure 13: The influence of the blade inlet angle on PAT power.

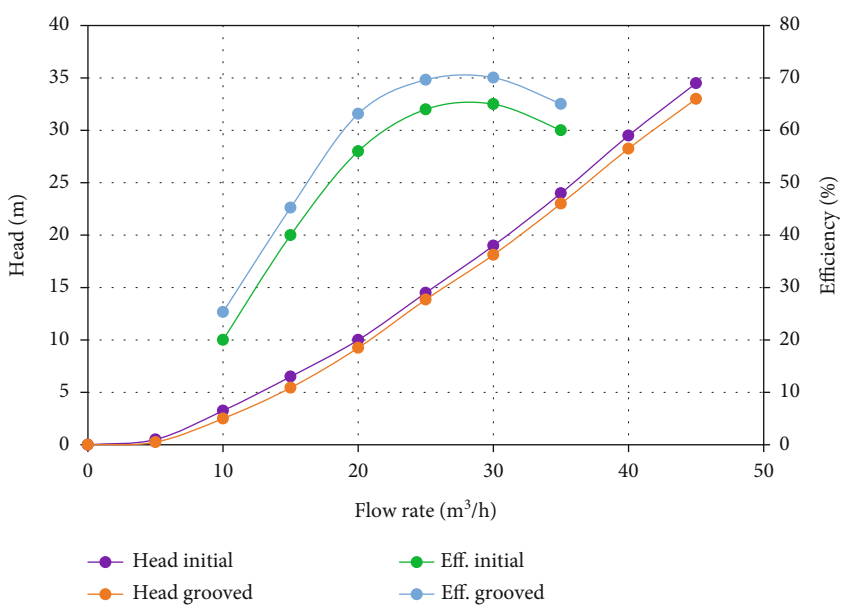

Figure 14: The influence of blade grooving on PAT efficiency.

stress tensor is defined by

$$\tau_{ij}^{R} = \mu_t \left(\frac{\partial u_i}{\partial x_j} + \frac{\partial u_j}{\partial x_i} - \frac{2}{3}\delta_{ij}\frac{\partial u_k}{\partial x_k} \right) - \frac{2}{3}\rho k \delta_{ij}. \quad (4)$$

The Kronecker delta function δij is equal to one when $i = j$ and zero otherwise, μ is the viscosity coefficient, k is the turbulent kinetic energy, and μt is the turbulent eddy viscosity coefficient:

$$\mu_t = f_u \frac{C_u \rho k^2}{\varepsilon}, \quad (5)$$

where ε is turbulent dissipation and f_u is a turbulent viscosity factor having the following form:

$$f_u = \left[1 - \exp\left(-0.0165 R_y\right)\right]^2 \bullet \left(1 + \frac{20.5}{R_T}\right), \quad (6)$$

with

$$R_T = \frac{\rho k^2}{\mu \varepsilon}, \quad (7)$$

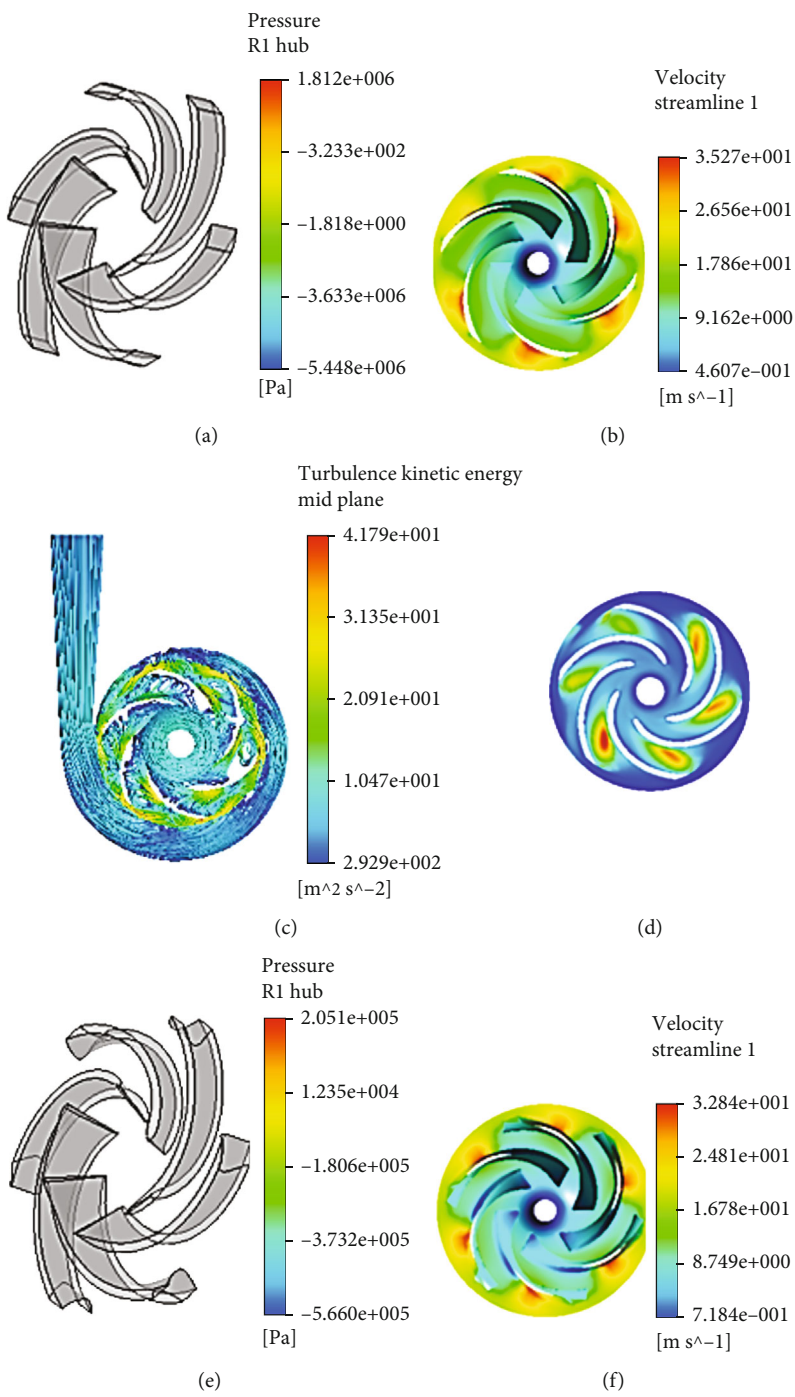

Figure 15: Continued.

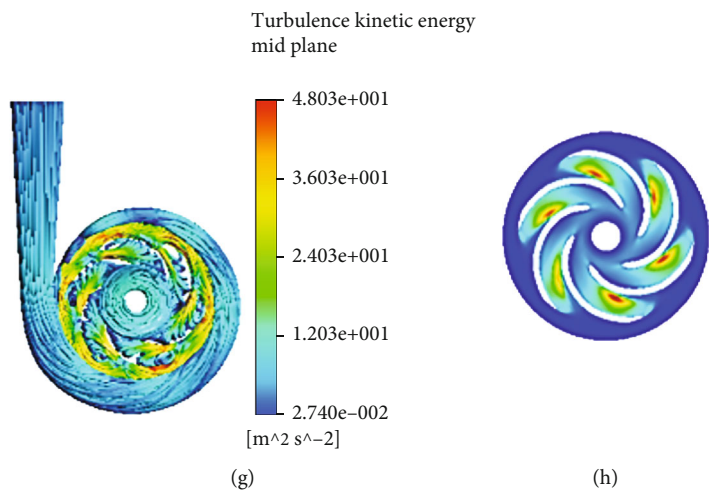

Figure 15: The effect of blade grooving on the internal flow characteristics of the PAT.

$$R_y = \frac{\rho\sqrt{ky}}{\mu}, \tag{8}$$

where y is the distance from the wall.

The first and second initial boundary conditions are specified as the total pressure at the inlet and the mass flow rate at the outlet [23, 24]. The interface is specified between the rotor and stator. The rest boundary conditions impeller and volute are defined as a rotating and stationary wall, respectively. Water at standard working conditions was used as a working fluid. The model description, operating conditions, materials, and boundary conditions are summarized in Table 2, which also lists the key assumptions used in the CFD simulation. Since the only independent variable in the current CFD simulation is mass flow rate, performance curves for the PAT were developed by varying the mass flow rate (Figure 3). All necessary parameters are specified as mathematical expressions in the parameter set module of Ansys CFX.

2.3. Construction of Experimental Setup. It is necessary to compare the simulated results with the experimental data to determine how accurate they are. Activities undertaken in the experimental study are designing, establishing the experimental test rig, and conducting the experiment.

A complete setup (Figure 4) consists of the following: (i) a feed pump with a power rating of three hp and a specific speed of 16 at the best efficiency point (BEP) was used to supply the required pressure and flow to the PAT. (ii) A low specific speed PAT, which delivered excessive pressure at a low flow rate, was taken into consideration. (iii) Polypropylene random pipes are used to circulate the water through the system. A bypass pipe was installed to control excess flow. Reducers/expanders had been wanted to attach the pipes having dissimilar sizes. (iv) Primary and secondary water tanks having a capacity of 420 and 320 liters are used as a water reservoir to provide sufficient water for the feed pump. Both tanks were joined by a pipe at the sidewall to keep the water at an optimum height. (v) Two gate valves placed in the piping line are used to control and vary the flow rate; the instantaneous pressure is measured by the pressure gauges. The system was hinged into the wall and the ground to absorb the shock when the experiment is performed.

The list of devices used to measure the performance parameters is tabulated in Table 3 along with the measurement range and principal error. After recording all parameters, input power (P_{in}), output power (P_{out}), and efficiency (η) of PATs were calculated using

$$P_{\text{in}} = \rho g Q_t H_{t,} \tag{9}$$

where ρ is the density of the water = 1000 kg/m^3, g is gravitational constant = 9.81 m/s^2, and Q_t is the flow rate of the PAT

$$P_{\text{out}} = \tau\omega, \tag{10}$$

where τ is torque developed by the shaft and ω is the angular velocity of the shaft.

$$\eta = \frac{P_{\text{out}}}{P_{\text{in}}}. \tag{11}$$

$$E_S = \sqrt{E_Q^2 + E_{H1}^2 + E_{H2}^2 + E_n^2 + E_F^2}. \tag{12}$$

To ensure the correctness of the experimental data, the average of ten repeated measurements was recorded for each of the performance parameters. According to [25–27], a first-order uncertainty analysis is carried out using the constant odds combination method, based on a 95 percent confidence level, where 3.1%, 3.2%, 2.4%, and 3.5% are respective uncertainties in flow rate, pressure head, power, and efficiency.

3. Result and Discussion

3.1. Comparison between Numerical and Experimental Results. The working behavior of PAT predicted by CFD and developed by experiment is presented in (Figure 3), in

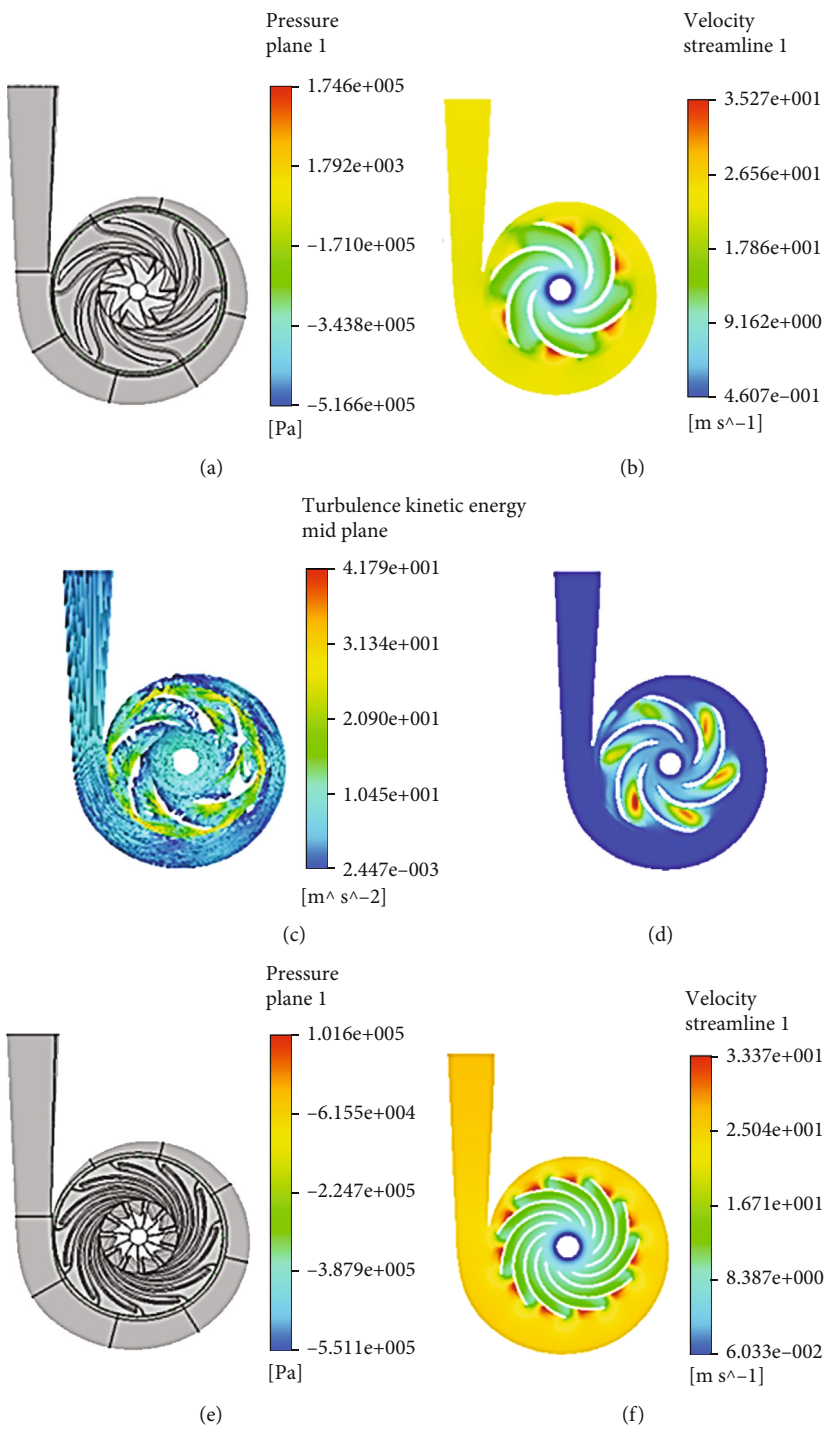

Figure 16: Continued.

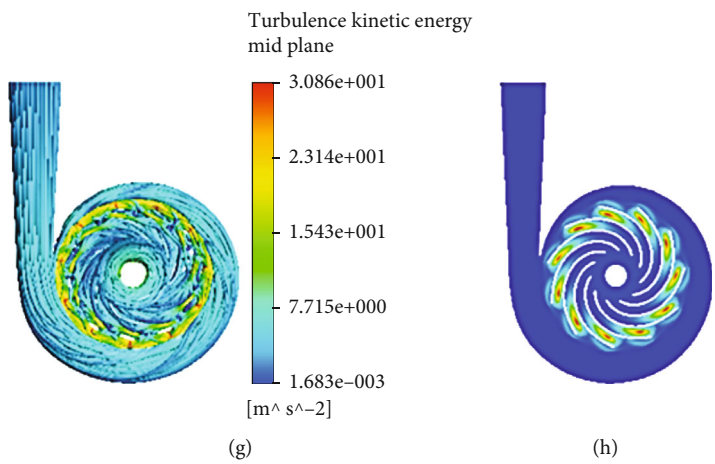

Figure 16: The impact of modification techniques on pressure distribution, velocity streamline, and turbulence kinetic energy.

which the capacity of the PAT increases with increasing pressure head and vice versa as expected. The BEP of the PAT is observed as the head of 17 m and the flow rate of 27.5 m^3/h; the power and efficiency of the PAT at this point are 850.33 W and 65.15%. Numerical errors always existed due to a convincing approximation of natural laws, and only hydraulic loss is considered in the simulation. Thus, the CFD results are slightly higher than the experimental test outputs. The deviation of CFD (Equation (13)) for pressure head, flow rate, output power, and efficiency at the BEPs is 2.94%, -1.82%, 2.88%, and 1.76%, respectively, and presented in Table 4. In all cases, the numerical result is found at an acceptable level.

$$\text{Percentage of deviation} = \frac{\text{Num.} - \text{Exp.}}{\text{Num.}} \times 100. \quad (13)$$

CFD is unable to simulate disc friction, mechanical losses, and leakage. Since the flow volume did not take into account the sealing gap or the space between pump components [7]. The volumetric efficiency η_v (Equation (14)), hydraulic efficiency η_h (Equation (15)), and mechanical efficiency η_m (Equation (16)) are identical to those of turbine and pump modes at the same rotational speed [28–30].

$$\eta_v = \frac{1}{1 + 0.68 n_s^{-2/3}}, \quad (14)$$

$$\eta_h = 1 - 0.08351 g \sqrt[3]{\frac{Q}{n}}, \quad (15)$$

$$\eta_m = 1 - 0.07 \frac{1}{n_s/100^{7/6}}, \quad (16)$$

$$\eta_{tot} = \eta_v \eta_h \eta_m. \quad (17)$$

Equations (14) through (16) give the value 0.91, 0.84, and 0.86 for volumetric, hydraulic, and mechanical efficiencies, respectively. The overall efficiency of the PAT (Equation (17)) equals 0.657, which is well agreed with the simulated value (Table 4).

3.2. Performance Improvement of the PAT. As discussed in the previous sections, impeller modification was the main parameter to improve the performance of the PAT. In this work also, the effect of the number of impellers, blade thickness, blade tip rounding, blade inlet angle, and blade grooving methods are investigated numerically; then compare the output with experimentally validated data. Finally, a simultaneous modification technique is applied to achieve maximum performance. The intention is to improve impeller and hydraulic losses, e.g., shock loss, incidence loss, surface friction loss, blade loading loss, separation loss, wake mixing loss, and recirculation loss [31, 32]. The internal hydraulic structure, output power, and overall efficiency are used as the performance evaluation parameters.

3.3. The Number of Impeller Blades. The blades of the hydraulic pump are usually lower in number than the hydraulic turbine. This is one of the factors which influence the pump's performance in turbine mode due to the excess distance between blades; this is the potential cause for flow separation within the flow passage. The effect of seven different blade numbers (6 up to12) on the performance of PAT is studied, while other parameters are kept the same as in Table 1.

Increasing the number of impeller blades has a positive effect on the performance of PAT; in this study, the maximum power, as well as efficiency, was found at blade number eleven (Figure 5). When the number of impeller blades of PAT increased from six to eleven, the efficiency improved from 65.15% to 69.94%. An impeller with 12 blades is the break-off point where the efficiency starts to diminish to 68.55%; the output power also starts to decrease at the same point. This indicates that a further increase in the number of blades will reduce the flow area, consequently decreasing the efficiency and output power generated by the impeller due to the increasing flow blockage effect.

The static pressure distribution in the mid-cross-section of the turbine model is shown in Figure 6. At the minimum blade number (i.e., $Z = 6$), the pressure among the blade is not uniformly distributed. However, by increasing the number of blades, this problem has been solved. The internal

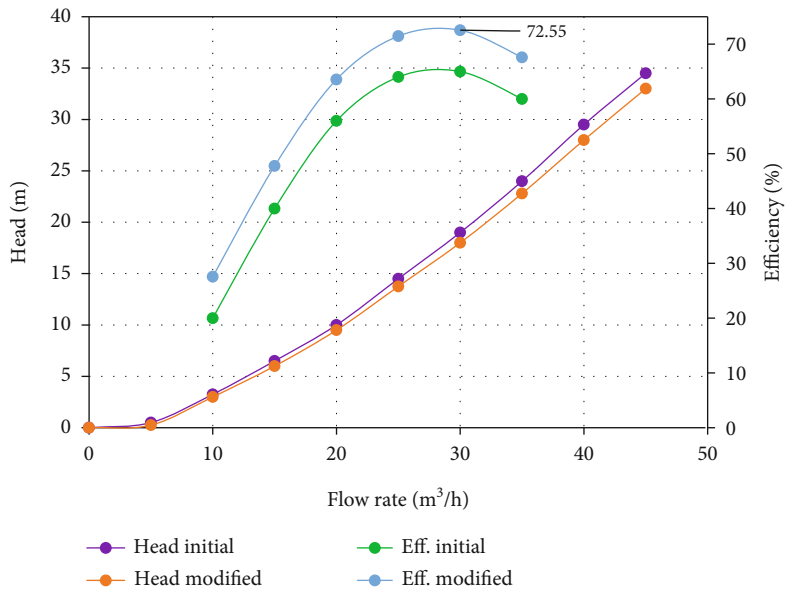

Figure 17: Simultaneous performance improvement of PAT.

Table 5: Comparison of the modification techniques.

Modification type	Power (W)	Efficiency (%)
Initial blade (unmodified)	850.33	65.15
Increasing the number of blades	902.00 (5.72%)	69.94 (6.85%)
Decreasing blade thickness	861.06 (1.24%)	66.89 (2.60%)
Blade tip rounding	864.30 (1.61%)	68.34 (4.66%)
Blade inlet angles	875.44 (2.86%)	69.58 (6.36%)
Blade grooving	895.24 (5.01%)	70.06 (7.00%)
Simultaneous	950.83 (10.56%)	72.55 (10.20%)

flow becomes stable after a blade number of 8 and more, this causes increasing the overall performance of PAT. The internal flow characteristic, i.e., pressure distribution conforms to the external behavior of flow through PAT (Figure 5). This indicates that a six-bladed impeller is insufficient for a turbine to function at its best efficiency. Generally speaking, the maximum pressure is found at the inlet of the PAT impeller, then, it decreases dramatically along the impeller flow passage, and the least pressure is found at the impeller eye. This great drop in static pressure is due to the energy transfer of high-pressure energy to PAT's mechanical power.

3.4. Blade Thickness. Blade thickness is an essential geometric parameter in the design of turbo-machinery. Figure 7 shows how the thickness of the blade gradually increases from the trailing edge to the leading edge in each case. For this work, the numerical value of maximum blade thicknesses is taken into consideration for performance comparison. To explore its effect on PAT's performance, a comparative study on four different blade thicknesses was carried out. The initial blade which has 8.4 mm thickness was compared with 6 mm, 4 mm, and 2 mm with the same decreasing tendency.

Figure 8 shows the effect of decreasing blade thickness on the power output at BEPs, the performance of the PAT varies with the variation of blade thickness, and the maximum value is taken at 4 mm. The efficiencies at BEP are 65.15%, 66.61%, 66.89%, and 66.73% for blade thicknesses of 8.4 mm, 6 mm, 4 mm, and 2 mm, respectively. Two mm is the cut-off point, and the efficiency, as well as power output, starts to decrease. From a fluid mechanics point of view, a thinner blade thickness leads to longer flow channels between the blades, which causes friction loss and wake formation as the fluid works on the surface of the impeller blade. But blade thickness has no significant impact on the performance when compared with other modification methods.

The difference in static pressure distribution between impellers with a blade thickness of 8.4 mm and others is presented in Figure 9. Changing the blade thickness cannot solve the nonuniformity pressure distribution among the six blades. The midplane pressure distribution also shows that variation in blade thickness has no significant effect on the performance of PAT.

3.5. Blade Tip Rounding. The pump blades' outer peripheral edges are sharp (Figure 10(a)); it is advantageous when the pump runs in the direct mode because the water travels radially outward on account of centrifugal force in the maximizing area. However, in reverse mode, the sharp edges may

lead to loss related to a shock wave, net flow separation, and excessive turbulence. In the current study, the blade's trailing edge is entirely rounded; i.e., the radius is equivalent to 50% of the impeller thickness, and it does not have a substantial impact on the overall diameter of the impeller.

The comparison of results acquired with and without blade tip rounding is presented in Figure 11. Blade tip rounding led to a decrease in the head at the same flow rate. Also, there is a significant increase in efficiency at and near BEP. At the same flow rate, blade tip rounding improved for pressure head, output power, and efficiency is -3.03%, 1.61%, and 4.66%, respectively. After blade tip rounding, the needed pressure head of the PAT is reduced, as indicated by the negative sign. The reason for the performance enhancement is the reduction of the hydraulic loss due to the rounding effect.

3.6. Adjusting Blade Inlet Angle. The shape of the impeller can be defined by the blade inlet, outlet, and wrap angles, while the blade inlet angle (β) is a very critical parameter for directing the flow in the appropriate direction (Figure 12). For simulation purposes, the initial blade angle (22.5°) and others (20, 17.5, and 15 degrees) are used for comparison. The remaining geometric parameters are the same as those listed in Table 1.

Figure 13 illustrates the variation of power and efficiency with different blade inlet angles; PAT produces the highest power when the blade inlet angle is 17.5°, in which the blade inlet angle decreases from 22.5 to 20 degrees and the efficiency at the BEP is improved by 4.43%. The primary cause of this performance difference is that changing the blade's inlet angle affects the flow attack angle, which changes the impact losses experienced by the impeller. In conclusion, the model with a 20° blade inlet angle provides the best performance in terms of efficiency. Further decreasing blade inlet angle leads to an increase in turbulence and velocity fluctuation due to inappropriate flow direction.

3.7. Blade Grooving. The new modification technique known as blade grooving is introduced in this research work. The blade inlet angle is kept 22.5°. Since blade grooving does not affect the blade inlet angle of the pump in reverse mode. To meet the required impeller strength, the radius of the U-shape groove kept half of the blade thickness. For comparison, the working conditions and geometric parameters are the same for both cases.

The initial output power of the pump running in turbine mode is increased by 44.91 W. The efficiency of the machine is also improved by 4.91% (Figure 14). This modification technique provides the maximum performance enhancement when compared with increasing the number of blades, decreasing blade thickness, blade tip rounding, and changing the blade inlet angle.

Figure 15 shows the effect of blade grooving on pressure distribution, velocity streamline, and turbulence intensity of the pump in revere mode. The maximum static pressure is found at the tip of the initial impeller (Figure 15(b)); this may be a possible cause for decreasing axial momentum. The greatest pressure area is slightly relocated to the blade's center after the blade was grooved (Figure 15(f)). Flow circulation occurred due to the relatively large adverse pressure gradient in the fluid flow direction (Figure 15(c)). From the basic theory of fluid dynamics, an adverse pressure gradient happens when the static pressure rises in the direction of water flow as shown in Figure 15(b). The issue of flow separation and circulation is not entirely resolved by the blade grooving approach. This indicates that additional study is necessary to determine the suitable groove shape. Turbulence intensity, which is the relative index used to assess the level of turbulence, does not have a direct correspondence with the performance of the PAT, but it can indicate the velocity fluctuation and characterize the flow conditions. From Figure 15(h), it can be seen that the internal turbulence intensity of the grooved model is smaller than the initial. Because of this, the flow in the PAT is more stable, which could affect the hydraulic performance of the PAT.

3.8. Simultaneous Modification. The application of two or more modification techniques is one of the feasible options to achieve the best performance. In addition to blade tip rounding and blade grooving, the best parameters are 11 blades, 20° blade inlet angle, and 4 mm blade thickness.

Analyzing the internal flow characteristic of the PAT is necessary to understand the performance variance between the initial and modified blade. From the impeller blade's middle section to the blade surface, the static pressure, velocity streamline, and turbulence kinetic energy distribution are shown in Figure 16. Large eddy forms between the impellers and flow separations are shown when the PAT is used without modification. These are possibly caused by the large distance between blades and the inappropriate angle of attack, respectively. The problem of large eddy formation can be solved by increasing the number of blades, and blade tip rounding and suitable blade inlet angle solve the flow separation problems. Qualitative results show that the internal turbulence intensity of the modified impeller is smaller (Figure 16(h)). Therefore, the flow in the PAT is more stable with less velocity fluctuation and the flow losses will be smaller after the application of modification techniques.

The comparison of the complete performance characteristics curve of the original and modified PAT at a specified flow rate is plotted in Figure 17. With the use of modification techniques, the required pressure head is reduced and the efficiency is raised. The efficiency of the PAT at its best efficiency point is 72.55%.

Table 5 depicts the impact of different modification methods on PAT performance. The largest percentage of power and efficiency enhancement is obtained in the case of increasing the number of blades and blade grooving, respectively. However, changing blade thickness has no significant impact on the performance. The power output and efficiency are increased by 1.24% and 2.60%, respectively; this is the least one when compared with others. After the application of modification techniques simultaneously, the power and efficiency are raised by 100.5 W and 7.4%. From this comparative study, it can be concluded that the

simultaneous modification technique is the best option to improve the performance of PAT.

$$\text{Performance improvement} = \frac{\text{Modified value} - \text{Initial value}}{\text{Modified value}} \times 100. \tag{18}$$

4. Conclusions

In the present study, the performance analysis of commercially available centrifugal pumps has been carried out to operate in reverse mode. Ansys CFX coupled with standard k-ε is used to analyze the performance. Then, the numerical outputs of the original PAT model were validated with experimental results. In the numerical analysis, increasing the number of blades, decreasing blade thickness, blade tip rounding, changing blade inlet angles, and blade grooving are considered parameters to conduct impeller modification. Then, those modification techniques are applied simultaneously to achieve maximum performance. Based on this, the following conclusions are drawn:

(i) The considered pump can operate satisfactorily as a turbine with an efficiency of 65.15%. The initial performance of PAT can be further enhanced using the key impeller parameter modifications

(ii) The maximum possible performances are achieved at 11 blades, 4 mm thick, blade tip rounding, 20^0 blade angle, and blade grooving; at this parameter, the efficiency is 69.94%, 66.89%, 68.34, 69.58%, and 70.06%, respectively

(iii) Among the five modification techniques, increasing the number of blades and blade grooving gives the maximum output for power and efficiency, respectively. But decreasing the blade thickness has no significant impact on the performance

(iv) Under the BEP condition, the efficiency of the PAT increased by 7.40%, and the output power was enhanced by 10.56% after the modifications were applied. Also, the chosen modification techniques have a significant influence on decreasing large eddy formation inside the flow channel, decreasing the hydraulic loss in the impeller, decreasing the required head, stabilizing the internal flow, and improving the overall performance of PAT

(v) When the simulation and experimental results are compared by considering the pressure head, flow rate, power, and efficiency, the deviation is found to be 2.94%, -1.82%, 2.88%, and 1.76%, respectively. In the end, a detailed economic analysis and feasibility study of the modified PAT for rural electrification can be a potential future research direction. Future work will also include, testing different groups of shapes for blade grooving to study its effect on the performance of PAT.

Abbreviations

BEP: Best efficiency point
CFD: Computational fluid dynamics
FVM: Finite volume method
g: Gravitational acceleration (m/s^2)
GDP: Gross domestic product
H: Head (m)
k: Turbulent kinetic energy (J/kg)
MHP: Micro-hydropower
P: Power (W)
PAT: Pump as turbine
PPR: Polypropylene random
Q: Flow rate (L/s)
RANS: Reynolds-averaged Navier-stokes
t: Blade thickness
z: Number of blade
η: Efficiency (%)
ρ: Density (kg/m^3)
ε: Turbulence dissipation
β: Blade inlet angle.

Data Availability

All data presented within the paper are available in a digital format upon request.

Conflicts of Interest

The authors declare that they have no known competing financial interests or personal relationships that could have appeared to influence the work reported in this paper.

Acknowledgments

The authors recognized the financial support by Addis Ababa Science and Technology University (AASTU) under internal research grants (Grant No. EM-229/19-1/21).

References

[1] D. Novara and A. McNabola, "A model for the extrapolation of the characteristic curves of pumps as turbines from a datum best efficiency point," *Energy Conversion and Management*, vol. 174, pp. 1–7, 2018.

[2] A. Bozorgi, E. Javidpour, A. Riasi, and A. Nourbakhsh, "Numerical and experimental study of using axial pump as turbine in Pico hydropower plants," *Renewable Energy*, vol. 53, pp. 258–264, 2013.

[3] M. A. Ismail, A. K. Othman, S. Islam, and H. Zen, "End suction centrifugal pump operating in turbine mode for microhydro applications," *Advances in Mechanical Engineering*, vol. 6, 2014.

[4] C. Valero, M. Egusquiza, E. Egusquiza, A. Presas, D. Valentin, and M. Bossio, "Extension of operating range in pump-turbines. Influence of head and load," *Influence of Head and Load, Energies*, vol. 10, no. 12, p. 2178, 2017.

[5] M. Simão, M. Pérez-Sánchez, A. Carravetta, and H. M. Ramos, "Flow conditions for PATS operating in parallel: experimental and numerical analyses," *Energies*, vol. 12, no. 5, pp. 901–919, 2019.

[6] A. N. Jemal and M. G. Haile, "Comprehensive Review of Pump as Turbine," *Renewable Energy and Sustainable Development*, vol. 5, pp. 68–79, 2019.

[7] X. Wang, J. Yang, Z. Xia, Y. Hao, and X. Cheng, "Effect of velocity slip on head prediction for centrifugal pumps as turbines," *Mathematical Problems in Engineering*, vol. 2019, Article ID 5431047, 10 pages, 2019.

[8] M. Rossi, M. Righetti, and M. Renzi, "Pump-as-turbine for energy recovery applications: the case study of an aqueduct," *Energy Procedia*, vol. 101, pp. 1207–1214, 2016.

[9] D. Zhou, H. Chen, and C. Yang, "A highly efficient Francis turbine designed for energy recovery in cooling towers," *Advances in Mechanical Engineering*, vol. 7, no. 3, 2015.

[10] D. Ram Adhikari, "The design of high efficiency crossflow hydro turbines: a review and extension," *Energies*, vol. 11, no. 2, p. 267, 2018.

[11] P. Singh and F. Nestmann, "Internal hydraulic analysis of impeller rounding in centrifugal pumps as turbines," *Experimental Thermal and Fluid Science*, vol. 35, no. 1, pp. 121–134, 2011.

[12] Y. Han and L. Tan, "Influence of rotating speed on tip leakage vortex in a mixed flow pump as turbine at pump mode," *Renewable Energy*, vol. 162, pp. 144–150, 2020.

[13] D. Jianguo, G. Chang, D. Adu, R. Darko, M. A. S. Khan, and E. O. Antwi, "Numerical simulation and computational flow characterization analyses of centrifugal pump operating as turbine," *Complexity*, vol. 2021, Article ID 9695452, 9 pages, 2021.

[14] S. S. Yang, F. Y. Kong, W. M. Jiang, and X. Y. Qu, "Effects of impeller trimming influencing pump as turbine," *Computers and Fluids*, vol. 67, pp. 72–78, 2012.

[15] M. Liu, L. Tan, and S. Cao, "Performance prediction and geometry optimization for application of pump as turbine: a review," *Frontiers in Energy Research*, vol. 9, pp. 1–16, 2022.

[16] M. A. I. Ismail, A. K. Othman, H. Zen, and M. S. Misran, "CFD modelling of pump as turbine with various number of blade for microhydro system," *Journal of Applied Science & Process Engineering*, vol. 3, no. 1, pp. 17–23, 2016.

[17] Y. Sun-Sheng, K. Fan-Yu, F. Jian-Hui, and X. Ling, "Numerical research on effects of splitter blades to the influence of pump as turbine," *International Journal of Rotating Machinery*, vol. 2012, Article ID 123093, 9 pages, 2012.

[18] S. S. Yang, C. Wang, K. Chen, and X. Yuan, "Research on blade thickness influencing pump as turbine," *Advances in Mechanical Engineering*, vol. 6, 2014.

[19] M. Simão, M. Pérez-Sánchez, A. Carravetta, P. López-Jiménez, and H. M. Ramos, "Velocities in a centrifugal PAT operation: experiments and CFD analyses," *Fluids*, vol. 3, no. 1, p. 3, 2018.

[20] M. A. Ismail, W. K. Muzammil, M. Rahman, M. W. K. Ibrahim, and S. Misran, "Experimental design and analysis of pump as turbine for microhydro system," *IOP Conference Series: Materials Science and Engineering*, vol. 217, p. 012014, 2017.

[21] M. Pérez-Sánchez, M. Simão, P. A. López-Jiménez, and H. M. Ramos, "CFD analyses and experiments in a pat modeling: pressure variation and system efficiency," *Fluids*, vol. 2, no. 4, p. 51, 2017.

[22] K. Kan, Z. Xu, H. Chen et al., "Energy loss mechanisms of transition from pump mode to turbine mode of an axial-flow pump under bidirectional conditions," *Energy*, vol. 257, p. 124630, 2022.

[23] N. K. Lin, M. M. Soe, and A. M. Thu, "Design, simulation and performance on the effect of modification on impeller tip for pump as turbine (PAT)," *International Journal of Scientific and Research Publications*, vol. 7, pp. 844–860, 2017.

[24] Y. Han and L. Tan, "Dynamic mode decomposition and reconstruction of tip leakage vortex in a mixed flow pump as turbine at pump mode," *Renewable Energy*, vol. 155, pp. 725–734, 2020.

[25] J. R. Taylor, *An Introduction to Error Analysis, Second edi*, University Science Books, Sausalito, California, 1997.

[26] S. J. Kline, "The purposes of uncertainty analysis," *ASME Journal of Fluids Engineering*, vol. 107, no. 2, pp. 153–160, 1985.

[27] R. J. Moffat, "Contributions to the theory of single-sample uncertainty analysis," *ASME Journal of Fluids Engineering*, vol. 104, no. 2, pp. 250–258, 1982.

[28] S. Huang, G. Qiu, X. Su, J. Chen, and W. Zou, "Performance prediction of a centrifugal pump as turbine using rotor-volute matching principle," *Renewable Energy*, vol. 108, pp. 64–71, 2017.

[29] L. Wang, S. N. Asomani, J. Yuan, and D. Appiah, "Geometrical optimization of pump-as-turbine (PAT) impellers for enhancing energy efficiency with 1-D theory," *Energies*, vol. 13, no. 16, p. 4120, 2020.

[30] P. C. I. J. Karassik, J. P. Messina, and C. C. Heald, *Pump Handbook*, The McGraw-Hill Companies, Inc, 4th Edition edition, 2008.

[31] M. Liu, L. Tan, and S. Cao, "Theoretical model of energy performance prediction and BEP determination for centrifugal pump as turbine," *Energy*, vol. 172, pp. 712–732, 2019.

[32] K. Kan, Z. Yang, P. Lyu, Y. Zheng, and L. Shen, "Numerical study of turbulent flow past a rotating axial-flow pump based on a level-set immersed boundary method," *Renewable Energy*, vol. 168, pp. 960–971, 2021.